DUAL RANGE DERINGING FOR NON-BLIND IMAGE DECONVOLUTION

Le Zou[†], *Howard Zhou*[‡], *Samuel Cheng*[§] *and Chuan He*[††]

[†]Visual Computing Group, Intel Corporation [‡]School of Interactive Computing, Georgia Institute of Technology

[§]School of Electrical and Computer Engineering, University of Oklahoma [††]Institute of Oil and Gas, Peking University

Email: le.zou@intel.com, howardz@cc.gatech.edu, samuel.cheng@ou.edu, CHe@pku.edu.cn

ABSTRACT

The popular Richardson-Lucy (*RL*) image deconvolution algorithm often produces undesirable ringing artifacts. In this paper, we propose a novel **Dual Range Deringing** (*DRD*) algorithm to address this problem. As a post-deconvolution scheme, the proposed approach follows RL deconvolution and removes ringing artifacts by utilizing information from both the input blurred image and the RL-deblurred image. DRD first marks smooth regions in the input blurred image that are likely to be subjected to ringing artifacts far away from any strong edge. It then identifies short-range ringing artifacts from the regions that surround strong edges in the RL-deblurred image. Once marked, both long- and short-range ringing artifacts are then suppressed by an edge-preserving deringing filter. We demonstrate the effectiveness of this procedure by performing experiments on a set of images blurred with various Point Spread Functions (*PSF*s). We compare DRD with state-of-the-art non-blind deconvolution algorithms and show that our results are virtually free of ringing artifacts with only minor detail losses. Moreover, DRD consists of computationally efficient local operations and is suitable for parallelization on modern GPUs.

1. INTRODUCTION

As a problem commonly found in many fields from consumer imaging to astronomy, image deblurring has attracted attentions from both academia and industry. When the blur kernel is known [1], the image deblurring problem is reduced to non-blind image deconvolution. But even when the blur kernel is given, it is still an ill-posed inverse problem, and obtaining high quality deblurring results remains a challenge. Many solutions have been proposed over the years. Among them, Richardson-Lucy deconvolution [2] has become a de facto approach due to its simplicity and high tolerance to noise. However, when blur kernels are large, RL deconvolution often produces noticeable ringing artifacts.

It is commonly believed that removing ringing artifacts directly from RL-deblurred results is very difficult [3]. Hence, most proposed approaches have been focusing on posting additional constraints. These techniques [3, 4] either requires limited blur kernel size or are computationally expensive. As an alternative, we show that it is possible to remove ringing artifacts on deblurred images while preserving important details. Our technique, Dual Range Deringing (DRD), acts as a post-deconvolution processing and removes ringing artifacts by utilizing information from both the input blurred image and the RL-deblurred image. As illustrated in Fig. 1. The idea is to mark locations that are likely to be subjected to ringing artifacts by exploiting both long- and short-range consequences from the deconvolution process. From the input blurred image, DRD marks large smooth regions where long-range ringing artifacts will be more noticeable after the deconvolution. The short-range ringing artifacts, by definition, are ringing artifacts that have not yet propagated far away from their source, strong edges, and these strong edges, are readily distinguishable even in an artifact-ridden deblurred image. DRD accomplishes both artifact marking tasks by standard edge detection, and once marked, ringing artifacts are suppressed by an effective edge-preserving deringing filter.

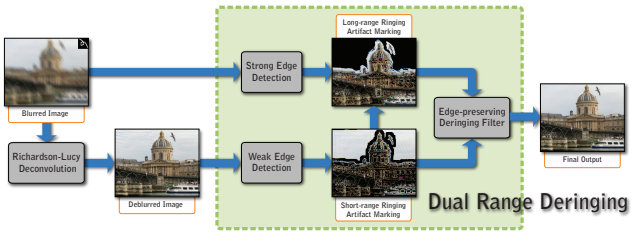

Fig. 1. Dual Range Deringing (DRD) as a post processing step to RL deconvolution for ringing artifacts removal.

Compared to the image deblurred by RL deconvolution (Fig. 2(RL)), the resulting image (Fig. 2(D)) is virtually free of ringing artifacts and remarkably few details are lost in the process. The close-up views also show separately the long-range (Fig. 2(LR)) and short-range (Fig. 2(SR)) ringing artifacts. Also included for reference are the original image (Fig. 2(O)) and deblurring result from a state-of-the-art non-blinded deconvolution algorithm [4] (Fig. 2(S)). The corresponding full image deblurring results can be found in Fig. 3. Our experiments indicate that, paired with standard RL-deconvolution, DRD can achieve deblurring results that are comparable to more sophisticated state-of-the-art algorithms [4], while requiring just a fraction of others' time. Moreover, since DRD consists of mostly local operations, it is readily parallelizable for even greater efficiency.

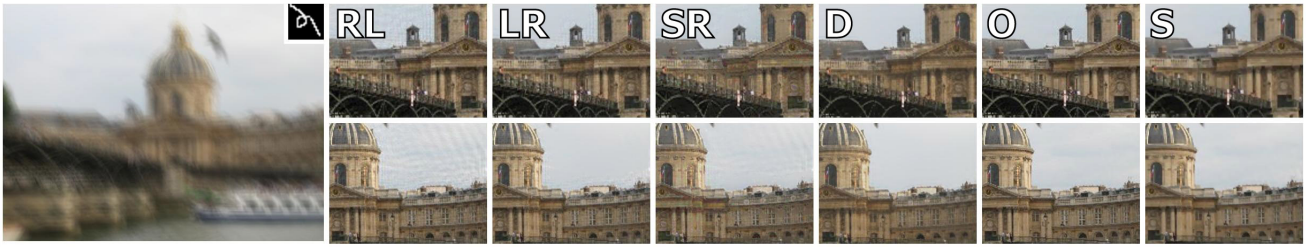

Fig. 2. Non-blind deconvolution example with a 31×31 blur kernel. From left to right: blurry image with the blur kernel, and non-blurry close-up views from : (RL) RL deconvolution result, (LR) RL result with Long-Range ringing suppressed, (SR) RL result with Short-Range ringing suppressed, (D) RL result after applying the complete DRD process, (O) Original image, and (S) result from Shan's algorithm [4].

2. RL DECONVOLUTION AND THE CAUSE OF RINGING ARTIFACTS

We first review RL deconvolution and explain the cause of its ringing artifacts. RL deconvolution is an iterative procedure that recovers a maximum likelihood solution of a latent image given its blurred version and the blur kernel. During each iteration, RL produces an estimate to the latent image based on the difference between its previous estimation and the input. It is robust to noise and computationally efficient. However, during the iteration process, the initial estimation error can accumulate and propagate. These errors often arise from regions near strong edges, and as the iteration proceeds, they propagate outwards from their source edges, manifesting as ringing artifacts. Based on their proximity to strong edges, in this paper, we classify these ringing artifacts as either short-range or long range. By definition, short-range ringing artifacts always appear near strong edges, and these strong edges are distinguishable even in poorly deblurred images. In contrast, long-range ringing artifacts are most noticeable when they appear in regions in the deblurred image that are mostly smooth, which also corresponds to smooth regions in the input blurred image. These two observations led us to our Dual Range Deringing (DRD) procedure, which we discuss in detail in the following section.

3. DUAL RANGE DERINGING

DRD effectively removes both long- and short-range ringing artifacts in three steps. 1) It identifies long-range ringing regions by examining the edge detection result of the input blurred image. The area where edge detector rarely fires are most likely. 2) It marks areas near strong edge response from the deblurred image as short-range ringing regions. Both step 1) and 2) require edge detection. In practice, we found that DRD works well with any reasonable edge detector, and we chose Sobel due to its simplicity. 3) Once all the regions where ringing artifacts are likely to reside are marked, DRD examines these regions one small window at a time, suppressing intensity anomalies if the window center is likely to coincide with a ringing artifact. Throughout these steps, DRD operates entirely in the spatial domain and requires only local information for deringing. As a result, DRD is computationally efficient and suitable for parallelization.

3.1. Long-Range Ringing Artifact Detection

Long-range ringing artifacts appear in smooth regions far away from strong edges when initial estimation errors propagate temporally during the RL deconvolution iterations. They are most noticeable to human eyes due to the strong contrast between their wave-like shape and the smooth background. To determine the location of such artifacts, we exam the edge detection result of the input blurred image and mark smooth regions that are far away from strong edge signals, because these are the areas where the long-range ringing artifacts will be most noticeable if they ever occur. This stage generates an intensity map LRM.

Algorithm 1 $Edge\_preserving\_deringing\_filter$(**I**, Δ_1, Δ_2,Δ_3 Σ_1,Σ_2, Σ_3, LRM, SRM)

for Each location (x, y) on **I** **do**
  Sum=0; Count=0;
  if ($\mathbf{LRM}(x, y) = 1$) **then**
    $\Delta = \Delta_1$; $\Sigma = \Sigma_1$;
  else
    if ($\mathbf{SRM}(x, y) = 1$) **then**
      $\Delta = \Delta_2$; $\Sigma = \Sigma_2$;
    else
      $\Delta = \Delta_3$; $\Sigma = \Sigma_3$;
    end if
  end if
  for $-\Delta \leq r1 \leq \Delta$ **do**
    for $-\Delta \leq r2 \leq \Delta$ **do**
      if ($|\mathbf{I}(x, y) - \mathbf{I}(x + r1, y + r2)| < \Sigma$) **then**
        Count = Count + 1; Sum = Sum + **I**(x+r1,y+r2);
      end if
    end for
  end for
  D(x,y) = (Sum + **I**(x,y))/(Count+1);
end for
Return D;

3.2. Short-Range Ringing Artifact Marking

After marking long-range ringing artifacts, only the unmarked locations will be considered for short-range ringing artifacts marking. We limit our search within a certain proximity R distance away from strong edges. Before applying RL deconvolution, these strong edges are blurred and mixed together in these areas. The initial errors at these locations typically have large values. Consequently, these locations are likely to contain strong ringing artifacts on the deblurred image. All locations within R will be examed since it is difficult to predict exactly where the ringing artifacts will occur. Also to prevent the deringing filtering from removing all details in the region, we only consider sites where the edge response value is below a certain threshold. This stage outputs a map SRM.

3.3. Edge-preserving Deringing Filtering

With both LRM and SRM ready, we apply our edge-preserving deringing filter at all marked locations to remove ringing artifacts. This procedure is described in Alg. 1. Within a certain range Δ of a marked location (x, y), the deringing filter collects its neighboring pixels where the intensity difference between the operating pixel $I(x, y)$ and its neighbors is below a certain threshold σ. Then the values of the collected pixels are summed up before being combined with the value of the operating pixel $I(x, y)$.

The input parameter Δ controls the range of the operating location for collecting pixels that are affected by ringing artifacts. Large scale ringing artifacts requires a large value of Δ. Since large blur kernel often results in large scale ringing artifacts, a large Δ is often necessary for large blur kernels. Normally we set its value to 5 to 12 depending on the blur kernel size. Furthermore, given an input image blurred with a certain kernel, different values of Δ are applied depending on whether short-range or long-range ringing artifacts are present. For short-range ringing artifacts, a smaller value of Δ will be enough because the scale of short-range ringing artifacts is much smaller compared to long-range ringing artifacts.

4. EXPERIMENTAL RESULTS

In this section, we validate the effectiveness of our proposed procedure by performing non-blind deconvolution on a set of images with various blur kernels. As a convention, all images are marked accordingly. Input blurred image be displayed with its corresponding blur kernel at its top right corner. The original image before blurring will be marked with a big **O** at its corner. Similarly, we use **RL** to mark results obtained after applying RL deconvolution, **T** - RL with Total Variation (*TV*) regularization [5] (with 50 iterations and 0.0016 as regularization factor), **S** - Expectation-maximization non-blind deblurring [4], and **D** for our Dual Range Deringing (DRD).

Fig. 3 shows three rows of scenery images. The first blur kernel is 21×21, and the other two are 39×39, which are large and of complex shapes. The results suggest that **D** (DRD) can effectively remove strong ringing artifacts exhibited in standard **RL** deconvolution results, making them comparable to results produced by **S**, a state-of-the-art algorithm. In fact, **S** has an overly diffusing effect in textured regions (See close-up comparisons in Fig 2, notice the window area and the railings on the bridge and the building). On the other hand, in regions where short-range ringing artifacts tangle with underlying texture, such as the ocean in the New York bank image, while **S** just blurs the texture, **D** sometimes overly suppresses the details, making underlying texture disappear altogether. In practice, both methods have exhibited more ringing artifacts on some images while performing better on others. Fig. 4 shows performance comparison on images used in [4]. Overall, DRD (**D**) exhibits more details than **S** at the price of tolerating more noise. We obtain all **S** results using author supplied parameters. The parameter settings for DRD (**D**) are omitted for space consideration. Speed-wise, without much optimization, **RL+D** typically requires less than half the time of **S**. We used the executable available from the author's website.

5. DISCUSSION AND CONCLUSION

To conclude, we have proposed a simple yet effective deringing scheme that complements RL deconvolution. As an efficient alternative to more sophisticated state-of-the-art non-blind deconvolution algorithms, our method can achieve remarkably good results. However, for certain images where the underlying texture is similar to the ringing artifacts, DRD can perform poorly and remove important details, such is the case with Picasso's wrinkles around his eyes. To resolve this deficiency will be our future work.

6. REFERENCES

[1] R. Fergus, B. Singh, A. Hertzmann, S. T. Roweis, and W. T. Freeman, "Removing camera shake from a single photograph," *ACM Trans. Graphics (SIGGRAPH)*, vol. 25, 2006.

[2] W. H. Richardson, "Bayesian-based iterative method of image restoration," *Journal of the Optical Society of America*, vol. 62, no. 1, pp. 55–59, 1972.

[3] L. Yuan, J. Sun, L. Quan, and H.-Y. Shum, "Progressive inter-scale and intra-scale non-blind image deconvolution," *ACM Trans. Graphics (SIGGRAPH)*, vol. 27, no. 3, 2008.

[4] Q. Shan, J. Jia, and A. Agarwala, "High-quality motion deblurring from a single image," *ACM Trans. Graphics (SIGGRAPH)*, vol. 27, no. 3, 2008.

[5] N. Dey, L. Blanc-Feraud, C. Zimmer, Z. Kam, J.-C. Olivo-Marin, and J. Zerubia, "A deconvolution method for confocal microscopy with total variation regularization," in *Proc. IEEE International Symposium on Biomedical Imaging*, Apr 2004.

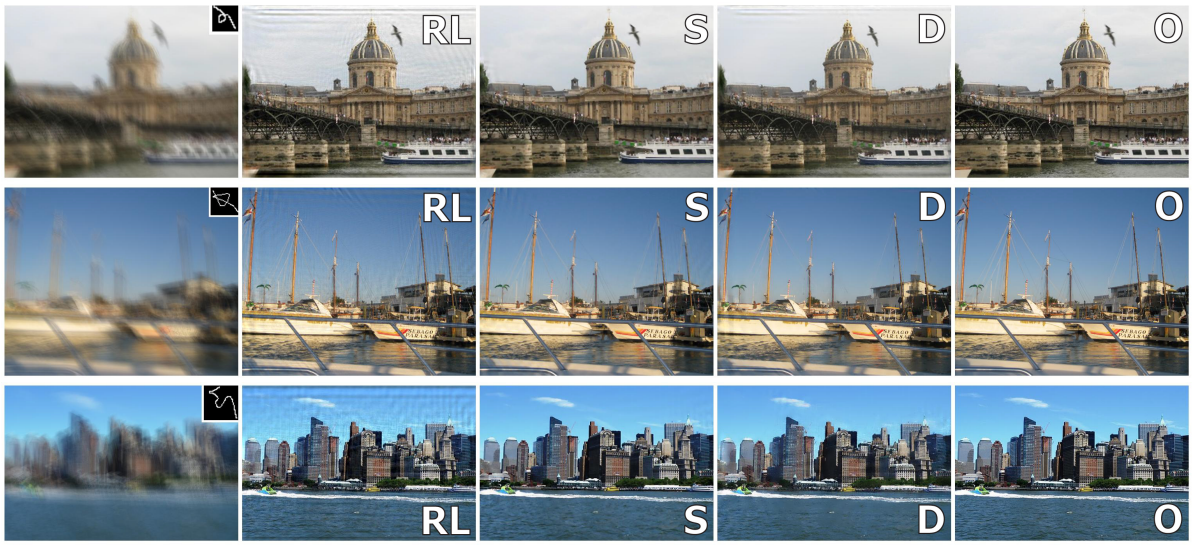

Fig. 3. Non-blind debeconvolution. From left to right: blurry images with their respective PSFs, (RL) deblurred images using standard RL deconvolution, (S) results from Shan et al. [4], (D) our results using standard RL deconvolution followed by DRD, and (O) original images.

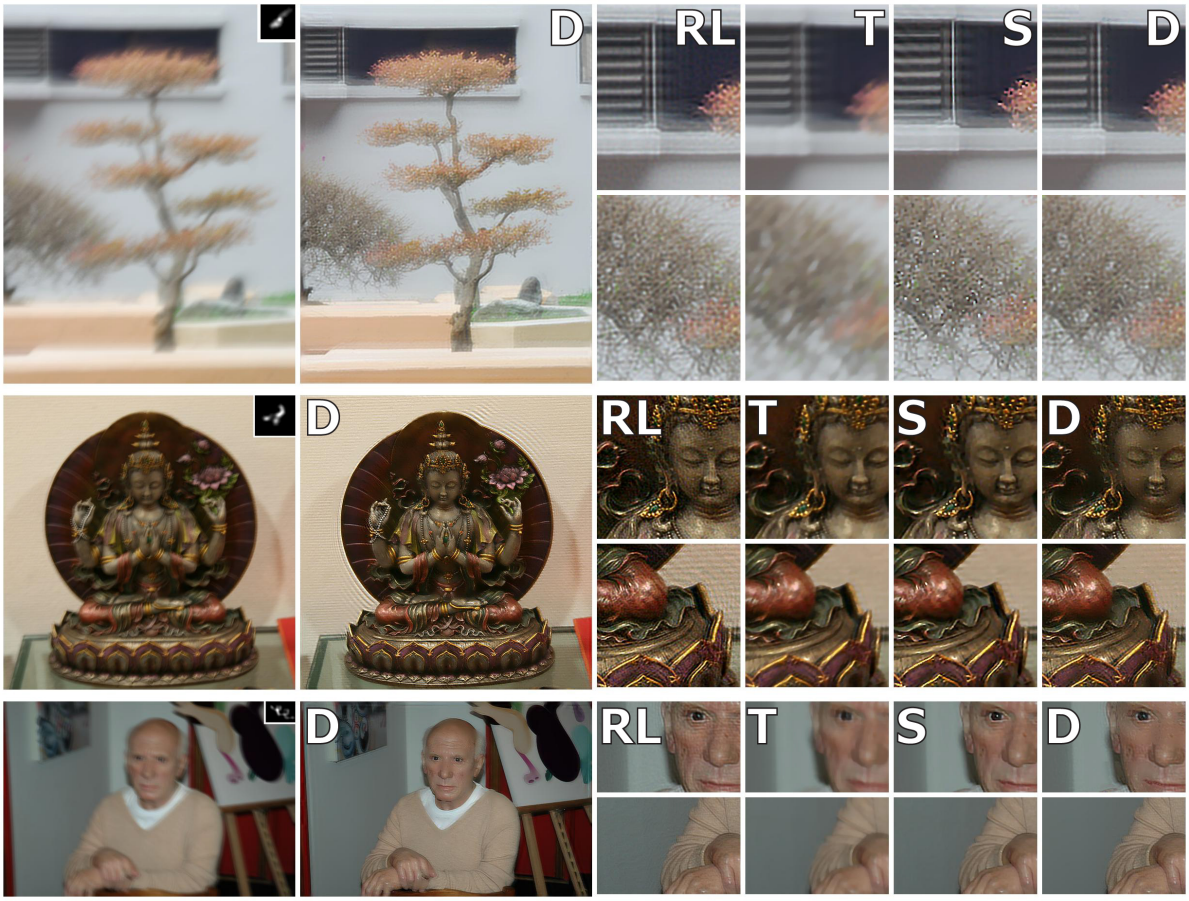

Fig. 4. Non-blind deconvolution images used in [4]. From left to right: blurry images with their respective PSFs, (D) our results using DRD, and close-up views from deblurred images using: (RL) RL deconvolution followed by DRD, (T) TV regularization, (S) Shan's algorithm [4], and (D) our results using RL followed by DRD. None of the original image is available.